

## Supplemental Experimental Procedures

### RNA Structural Analysis

RNA secondary structures were determined by SHAPE and DMS chemical probing experiments using previously described protocols for long non-coding RNAs (Novikova et al., 2012). The tertiary structure model was constructed using in-house RNA homology software based on structural motif libraries (Tung et al., 2002).

**SHAPE and DMS Chemical Probing:** RNA design and chemical probing experiments of *MALAT1* were performed in a similar manner as described previously (Novikova et al., 2012). Shortly, dsDNA templates for RNA synthesis were designed to carry a T7 promoter region and generated by PCR from DNA ultramers (IDT DNA Technologies, Coralville, IA). An additional sequence (structural cassette) GCGATCCGCTTCGGCGGATCCAAATTGGGCTTCGGTTCGGTTCGAT has been included at the 3'-end to provide a specific primer-binding site for chemical probing analysis. RNA was then synthesized by run-off transcription from these dsDNA templates using the T7-scribe Standard RNA IVT kit (Cellscript, Madison, WI). RNA products were extracted with phenol-chloroform and precipitated with 3M sodium acetate, pH=5.2, and ethanol.

In all chemical probing experiments, RNA was first denatured in water at 94°C for 2 min, snap-cooled on ice and then folded in HEPES buffer (50mM HEPES-KOH, pH=8.0, 100mM KCl) with 6mM MgCl<sub>2</sub> or without MgCl<sub>2</sub> for 30 min at 37°C. In all probing reactions, the final concentration of RNA was adjusted to 150 nM. SHAPE probing was done by treating folded RNA with 1M7 reagent (dissolved in DMSO) to a final concentration of 3 mM and by further incubating the sample for 5 min at 25°C. To obtain an unmodified RNA control, the 1M7 reagent was substituted with pure DMSO. Modified

(SHAPE) and unmodified ('blank') RNA were then purified separately using standard sodium acetate/ethanol procedure.

In DMS probing experiments, 1/20<sup>th</sup> volume of 10% DMS in ethanol was added to folded RNA. The sample was incubated on ice for 1 hour and quenched with 1/28<sup>th</sup> volume of  $\beta$ -mercaptoethanol (14M), 1/10<sup>th</sup> volume of 5M sodium acetate, pH=5.2, and 2.5 volumes of 100% ethanol. The mixture was incubated on ice for 15 min and centrifuged. The pellet was washed with 70% ethanol, dried and re-suspended in water. For unmodified RNA, DMS was substituted with 100% ethanol.

Modification sites of RNA were analyzed by reverse transcription and capillary electrophoresis. Reverse transcription was performed with an Alexa488-labelled primer, designed to anneal to a portion of the structural cassette, and Superscript III reverse transcriptase (Invitrogen). This was performed in the following manner: 4 pmoles of modified (SHAPE/DMS) or unmodified RNA (2  $\mu$ l) were mixed with 1.5 pmoles of Alexa488-primer (0.75  $\mu$ l), 1  $\mu$ l of dNTPs mix (2.5mM each) and 1.25  $\mu$ l of water. The mixture was incubated for 5 min at 65°C and then placed on ice. Afterwards, 2  $\mu$ l of Reverse transcription buffer (4 parts of 5XFirst Strand buffer and 1 part of 0.1M DTT supplied with the enzyme) and 1  $\mu$ l of Superscript III (200 U/ $\mu$ l) were added to the mixture. The mixture was incubated for 1 hour at 56°C and then for 10 min at 70°C. The reaction volume was then adjusted to 50  $\mu$ l with water and spin-washed using Bio-gel P6 (Bio-Rad) to remove salts. For assignment of nucleotide positions, two parallel dideoxy sequencing reactions (for A and C nucleotides) were carried out. The conditions for reverse transcription using dideoxy nucleotides were as above with the following exceptions: 1) the RNA was not folded or treated with any reagent, and 2) water was substituted with 1  $\mu$ l of 1 mM ddNTP (ddTTP for A-sequencing and ddGTP for C-sequencing).

To resolve cDNA products, 1  $\mu$ l of desalted solution was mixed with 20  $\mu$ l of deionized formamide, heated for 3 min at 94°C, placed on ice and further loaded on the 50 cm capillary of an ABI PRISM 3100-Avant genetic analyzer. The collected traces were manually aligned and Gaussian integrated. Reverse transcription stops observed in the blank traces were subtracted from the probing traces. The SHAPE and DMS traces were further normalized by averaging reactivities for highly reactive nucleotides in a way that the reactivities span 0 to 1.5 range.

**Tertiary Structure:** A model of the triplex tertiary structure was constructed using previously developed RNA homology software (Tung et al., 2002). The method uses an RNA structural motif library generated from the protein databank (PDB). In the case of the human triplex RNA system, a GC base pair is embedded in the middle of the triplex. The triplex was treated as two segments (65-70/143-149/111-117 and 71-74/150-153/107-110) linked at the bulge containing the GC pair. Each of the segments was modeled using the human telomerase RNA (protein databank accession code: 2K96) as a template. The two segments were docked to ensure the quality of the stereochemistry of the phosphate linkages and to preserve base stacking. The structure of the long stem-loop (residues 75-106) was directly modeled using the RNA motif library.

### **Animal and Cell Culture**

All animal protocols have been approved by the CSHL Animal Care and Use Committee. Mature male and female *Anolis carolinensis* were purchased from Carolina Biological Supply Company (Burlington, NC). Animals were euthanized, and organs or tissues were collected and freshly frozen in liquid nitrogen, and stored in -80°C.

U2OS (human, ATCC HTB-96), C2C12 (mouse, ATCC CRL-1772), IgH-2 (lizard, ATCC CCL-108), A6 (*Xenopus*, ATCC CCL-102), and ZFL (zebrafish, ATCC CRL-2643)

cell lines was purchased from ATCC (Manassas, VA) and cultured in Dulbecco's Modified Eagle's Medium (DMEM) with 10% fetal bovine serum and non-essential amino acids under an instructed temperature.

### **Immunoblot Analysis**

Organs or tissues were lysed in 1X RIPA buffer (20mM Tris pH7.5, 150mM NaCl, 1mM EDTA, 1mM EGTA, 1%NP-40, 0.5% NaDoC, 0.1% SDS) containing 1x protease inhibitor (Sigma, MO) and 1X phosphatase inhibitor (Sigma, MO), and homogenized. The lysates were cleared by centrifugation. Protein concentration was measured using the DC<sup>TM</sup> protein assay kit (Bio-Rad, CA). A total 20 ug protein was separated on a 10% SDS PAGE (sodium dodecyl sulfate polyacrylamide gel electrophoresis) gel and probed by immunoblot using rabbit polyclonal anti-LIWI2 peptide 2 antibody (1:200, in house, Primmbiotech Inc., MA).

### **Generation of Polyclonal Antibody Against Lizard LIWI2**

Rabbit anti-LIWI2 polyclonal antibodies were raised using RLKAALVYNHPVFKG-Cys (LIWI2 peptide 1: 161-175 aa) and IHREPSLELADKLYY-Cys (LIWI2 peptide 2: 866-880 aa) Primmbiotech inc., MA). The same peptide was crosslinked to a solid support by using SulfoLink coupling Gel (Pierce Biotechnology, IL) and used for affinity purification of antibodies from serum. The rabbit polyclonal anti-LIWI2 peptide 2 specifically recognizes a protein with an expected size of LIWI2 only present in testis when used in immunoblot analysis, and also specifically labels male germ cells when used in immunofluorescent (IF) labeling analysis. Addition of LIWI2 peptide 2 abolishes the specific interaction detected by immunoblot and IF labeling analyses. Currently, we do not have the LIWI2 cDNA cloned and further analyses using overexpressed LIWI2 in cultured cells was not pursued.

### **RNA Fluorescent In Situ Hybridization (FISH) and Quantitative RT-PCR**

RNA FISH using nick-translated cDNA probes, and qRT-PCR, were performed as previously described (sequence information in Supplementary Data SF14) (Mao et al., 2011; Sunwoo et al., 2009). For qRT-PCR, target genes were analyzed using standard curves to determine relative levels of gene expression. The level of specific mRNAs was analyzed using a StepOne Real-Time PCR System (Applied Biosystems, CA). Individual RNA samples were normalized according to the level of *Gapdh*.

### **Ligation-based Cloning of the 3'-end of *mascRNA***

Cloning of *mascRNA* 3' end was performed as described previously (Wilusz et al., 2008). Briefly, the Modban oligo (IDT DNA Technologies, Coralville, IA) was ligated to the 3' ends of total RNA, reverse transcribed, nested-PCR amplified, and cloned to the pCR2.1 vector (Invitrogen, Calsbad, CA), and sequenced.

### **Chromatin RNA Immunoprecipitation (ChRIP)**

ChRIP was performed on lizard testis as has been described previously (Chiesa et al., 2012) with antibodies raised against core histone H3 (Ab1791, Abcam, Cambridge, MA), LIWI2 (in house), and rabbit IgG (Millipore, Billerica, MA). Briefly, lizard testis was cross-linked in 1% formaldehyde for 10 minutes at RT followed by 2M Glycine treatment at RT for 5 minutes, lysed in 1xPBS with 1mM MgCl<sub>2</sub> and 0.5% TritonX-100, washed in 1xPBS with 1 mM MgCl<sub>2</sub> with protease inhibitor and RNase inhibitor, resuspended in incubation buffer (50mM NaCl, 20mM Tris pH7.5, 5mM EDTA) and sonicated, and immunoprecipitated with antibodies described above. The immunoprecipitated RNA was de-crosslinked from chromatin by incubation at 55°C for 2 hours, and purified using phenol–chloroform, DNase-treated and re-purified by the phenol–chloroform method.

cDNA was synthesized using a Reverse Transcriptase Kit (Promega, Madison, WI).

*TancRNA*, Malat1, GAPDH, and  $\beta$ -Actin transcripts were measured by qPCR using the primers listed in Supplementary Data SF14.

### References:

Chiesa, N., De Crescenzo, A., Mishra, K., Perone, L., Carella, M., Palumbo, O., Mussa, A., Sparago, A., Cerrato, F., Russo, S., *et al.* (2012). The KCNQ1OT1 imprinting control region and non-coding RNA: new properties derived from the study of Beckwith-Wiedemann syndrome and Silver-Russell syndrome cases. *Hum Mol Genet* *21*, 10-25.

Mao, Y.S., Sunwoo, H., Zhang, B., and Spector, D.L. (2011). Direct visualization of the co-transcriptional assembly of a nuclear body by noncoding RNAs. *Nat Cell Biol* *13*, 95-101.

Novikova, I.V., Hennelly, S.P., and Sanbonmatsu, K.Y. (2012). Structural architecture of the human long non-coding RNA, steroid receptor RNA activator. *Nucleic Acids Res* *40*, 5034-5051.

Sunwoo, H., Dinger, M.E., Wilusz, J.E., Amaral, P.P., Mattick, J.S., and Spector, D.L. (2009). MEN epsilon/beta nuclear-retained non-coding RNAs are up-regulated upon muscle differentiation and are essential components of paraspeckles. *Genome research* *19*, 347-359.

Tung, C.S., Joseph, S., and Sanbonmatsu, K.Y. (2002). All-atom homology model of the Escherichia coli 30S ribosomal subunit. *Nat Struct Biol* *9*, 750-755.

Wilusz, J.E., Freier, S.M., and Spector, D.L. (2008). 3' end processing of a long nuclear-retained noncoding RNA yields a tRNA-like cytoplasmic RNA. *Cell* *135*, 919-932.

### Photo References:

Photos used in the graphical abstract are from the following:

Human: the Vitruvian Man, by Leonardo da Vinci

Chicken (NHGRI Press Photos): [https://urldefense.proofpoint.com/v2/url?u=http-3A\\_\\_genome.ucsc.edu\\_cgi-2Dbin\\_hgGateway-3Fhgsid-3D587104865-5FcGY8h2Hswkrdx0wLrPdvhPOQ2j8o&d=DwIFAg&c=mkpgQs82XaCKlwNV8b32dmVOmERqJe4bBOtF0CetP9Y&r=l16xslwarKb0qW3t50aEZA&m=5NoORJWsM58UzqS\\_EUX94waCaoTrOSsIRSsx65KJXe0&s=BEnglc3iXysp1qAqfb1DCm4WsAA9n5XyQNsJVj4TBFU&e=](https://urldefense.proofpoint.com/v2/url?u=http-3A__genome.ucsc.edu_cgi-2Dbin_hgGateway-3Fhgsid-3D587104865-5FcGY8h2Hswkrdx0wLrPdvhPOQ2j8o&d=DwIFAg&c=mkpgQs82XaCKlwNV8b32dmVOmERqJe4bBOtF0CetP9Y&r=l16xslwarKb0qW3t50aEZA&m=5NoORJWsM58UzqS_EUX94waCaoTrOSsIRSsx65KJXe0&s=BEnglc3iXysp1qAqfb1DCm4WsAA9n5XyQNsJVj4TBFU&e=)

Lizard: [https://urldefense.proofpoint.com/v2/url?u=http-3A\\_www.dpchallenge.com\\_image.php-3FIMAGE-5FID-3D18556&d=DwIFAg&c=mkpgQs82XaCKIwNV8b32dmVOmERqJe4bBOtF0CetP9Y&r=I16xslwarKb0qW3t50aEZA&m=5NoORJWsM58UzqS\\_EUX94waCaoTrOSsIRSsx65KJXe0&s=Q8kHvIhj37oHf9taRviJEQUKGcyIjwXhVfZQKhbfuvE&e=](https://urldefense.proofpoint.com/v2/url?u=http-3A_www.dpchallenge.com_image.php-3FIMAGE-5FID-3D18556&d=DwIFAg&c=mkpgQs82XaCKIwNV8b32dmVOmERqJe4bBOtF0CetP9Y&r=I16xslwarKb0qW3t50aEZA&m=5NoORJWsM58UzqS_EUX94waCaoTrOSsIRSsx65KJXe0&s=Q8kHvIhj37oHf9taRviJEQUKGcyIjwXhVfZQKhbfuvE&e=)

Zebrafish (NHGRI Press Photos): [https://urldefense.proofpoint.com/v2/url?u=http-3A\\_genome.ucsc.edu\\_cgi-2Dbin\\_hgGateway-3Fhgsid-3D587104865-5FcGY8h2Hswkrdx0wLrPdvhPOQ2j8o&d=DwIFAg&c=mkpgQs82XaCKIwNV8b32dmVOmERqJe4bBOtF0CetP9Y&r=I16xslwarKb0qW3t50aEZA&m=5NoORJWsM58UzqS\\_EUX94waCaoTrOSsIRSsx65KJXe0&s=BEnglc3iXysp1qAqfb1DCm4WsAA9n5XyQnsjVj4TBFU&e=](https://urldefense.proofpoint.com/v2/url?u=http-3A_genome.ucsc.edu_cgi-2Dbin_hgGateway-3Fhgsid-3D587104865-5FcGY8h2Hswkrdx0wLrPdvhPOQ2j8o&d=DwIFAg&c=mkpgQs82XaCKIwNV8b32dmVOmERqJe4bBOtF0CetP9Y&r=I16xslwarKb0qW3t50aEZA&m=5NoORJWsM58UzqS_EUX94waCaoTrOSsIRSsx65KJXe0&s=BEnglc3iXysp1qAqfb1DCm4WsAA9n5XyQnsjVj4TBFU&e=)

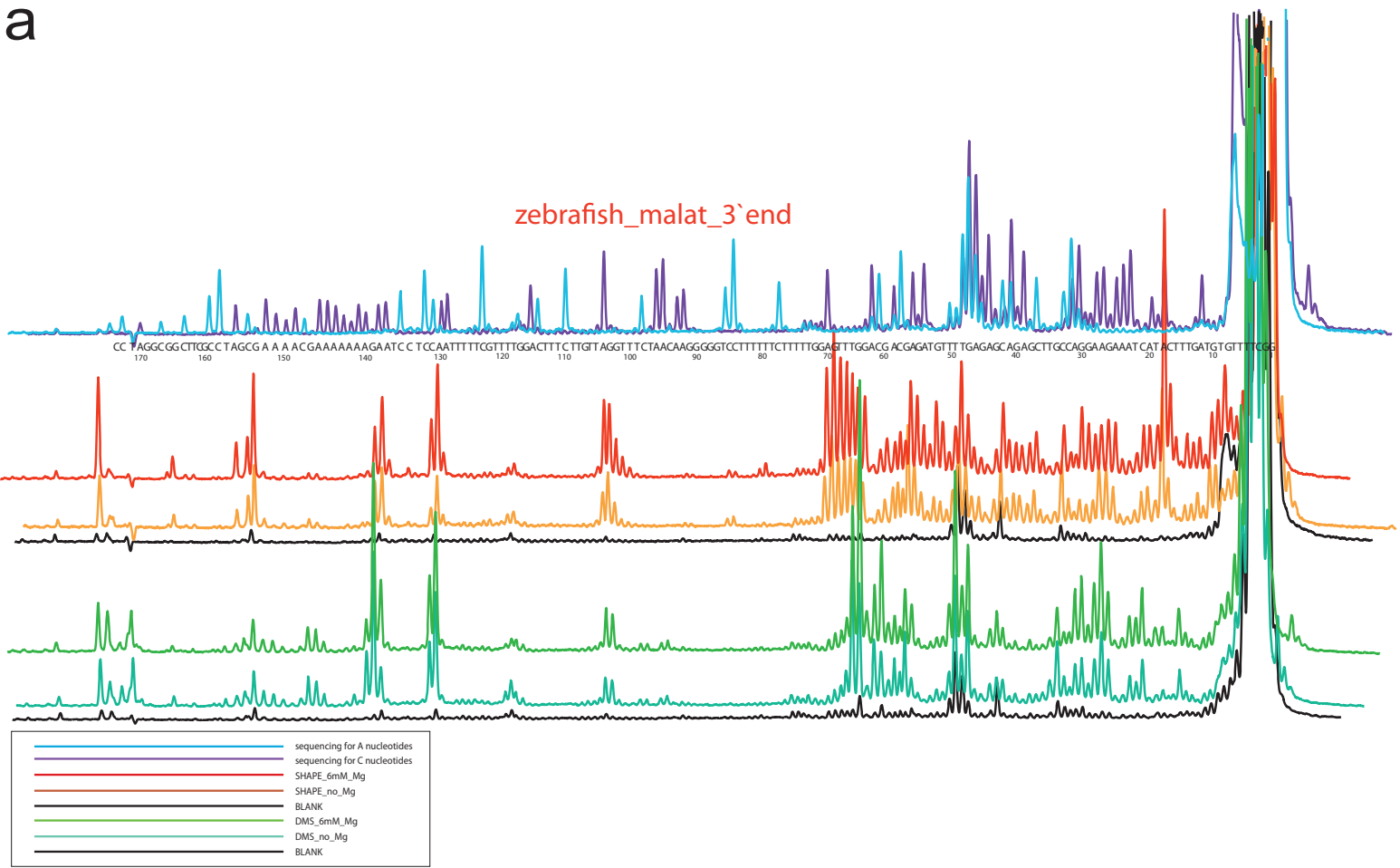
Medaka (Photo courtesy of Shinichi Morishita):

[https://urldefense.proofpoint.com/v2/url?u=http-3A\\_genome.ucsc.edu\\_cgi-2Dbin\\_hgGateway-3Fhgsid-3D587104865-5FcGY8h2Hswkrdx0wLrPdvhPOQ2j8o&d=DwIFAg&c=mkpgQs82XaCKIwNV8b32dmVOmERqJe4bBOtF0CetP9Y&r=I16xslwarKb0qW3t50aEZA&m=5NoORJWsM58UzqS\\_EUX94waCaoTrOSsIRSsx65KJXe0&s=BEnglc3iXysp1qAqfb1DCm4WsAA9n5XyQnsjVj4TBFU&e=](https://urldefense.proofpoint.com/v2/url?u=http-3A_genome.ucsc.edu_cgi-2Dbin_hgGateway-3Fhgsid-3D587104865-5FcGY8h2Hswkrdx0wLrPdvhPOQ2j8o&d=DwIFAg&c=mkpgQs82XaCKIwNV8b32dmVOmERqJe4bBOtF0CetP9Y&r=I16xslwarKb0qW3t50aEZA&m=5NoORJWsM58UzqS_EUX94waCaoTrOSsIRSsx65KJXe0&s=BEnglc3iXysp1qAqfb1DCm4WsAA9n5XyQnsjVj4TBFU&e=)

Lamprey (Photo courtesy of U.S. Environmental Protection Agency):

[https://urldefense.proofpoint.com/v2/url?u=http-3A\\_genome.ucsc.edu\\_cgi-2Dbin\\_hgGateway-3Fhgsid-3D587104865-5FcGY8h2Hswkrdx0wLrPdvhPOQ2j8o&d=DwIFAg&c=mkpgQs82XaCKIwNV8b32dmVOmERqJe4bBOtF0CetP9Y&r=I16xslwarKb0qW3t50aEZA&m=5NoORJWsM58UzqS\\_EUX94waCaoTrOSsIRSsx65KJXe0&s=BEnglc3iXysp1qAqfb1DCm4WsAA9n5XyQnsjVj4TBFU&e=](https://urldefense.proofpoint.com/v2/url?u=http-3A_genome.ucsc.edu_cgi-2Dbin_hgGateway-3Fhgsid-3D587104865-5FcGY8h2Hswkrdx0wLrPdvhPOQ2j8o&d=DwIFAg&c=mkpgQs82XaCKIwNV8b32dmVOmERqJe4bBOtF0CetP9Y&r=I16xslwarKb0qW3t50aEZA&m=5NoORJWsM58UzqS_EUX94waCaoTrOSsIRSsx65KJXe0&s=BEnglc3iXysp1qAqfb1DCm4WsAA9n5XyQnsjVj4TBFU&e=) .

a



b

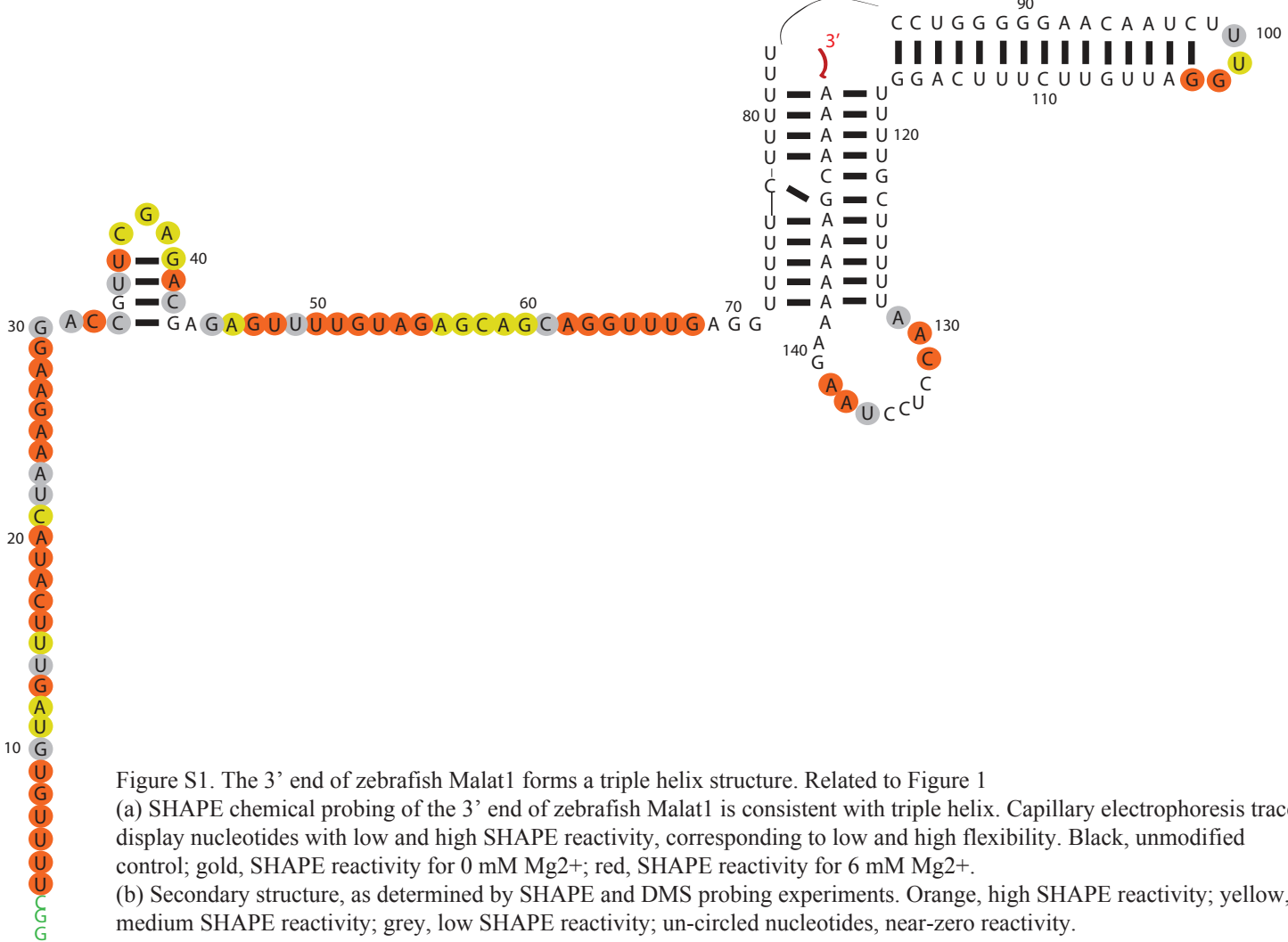


Figure S1. The 3' end of zebrafish Malat1 forms a triple helix structure. Related to Figure 1  
 (a) SHAPE chemical probing of the 3' end of zebrafish Malat1 is consistent with triple helix. Capillary electrophoresis traces display nucleotides with low and high SHAPE reactivity, corresponding to low and high flexibility. Black, unmodified control; gold, SHAPE reactivity for 0 mM Mg<sup>2+</sup>; red, SHAPE reactivity for 6 mM Mg<sup>2+</sup>.  
 (b) Secondary structure, as determined by SHAPE and DMS probing experiments. Orange, high SHAPE reactivity; yellow, medium SHAPE reactivity; grey, low SHAPE reactivity; un-circled nucleotides, near-zero reactivity.





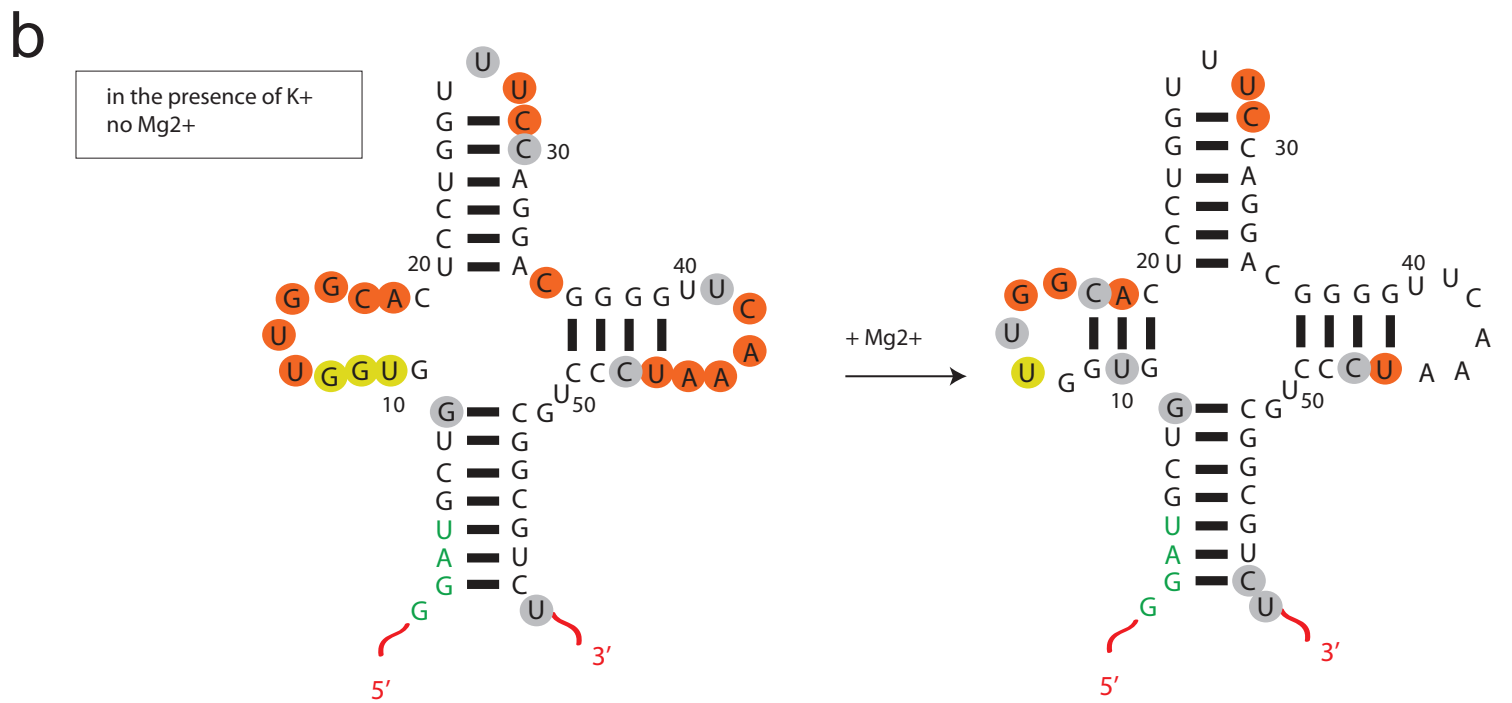
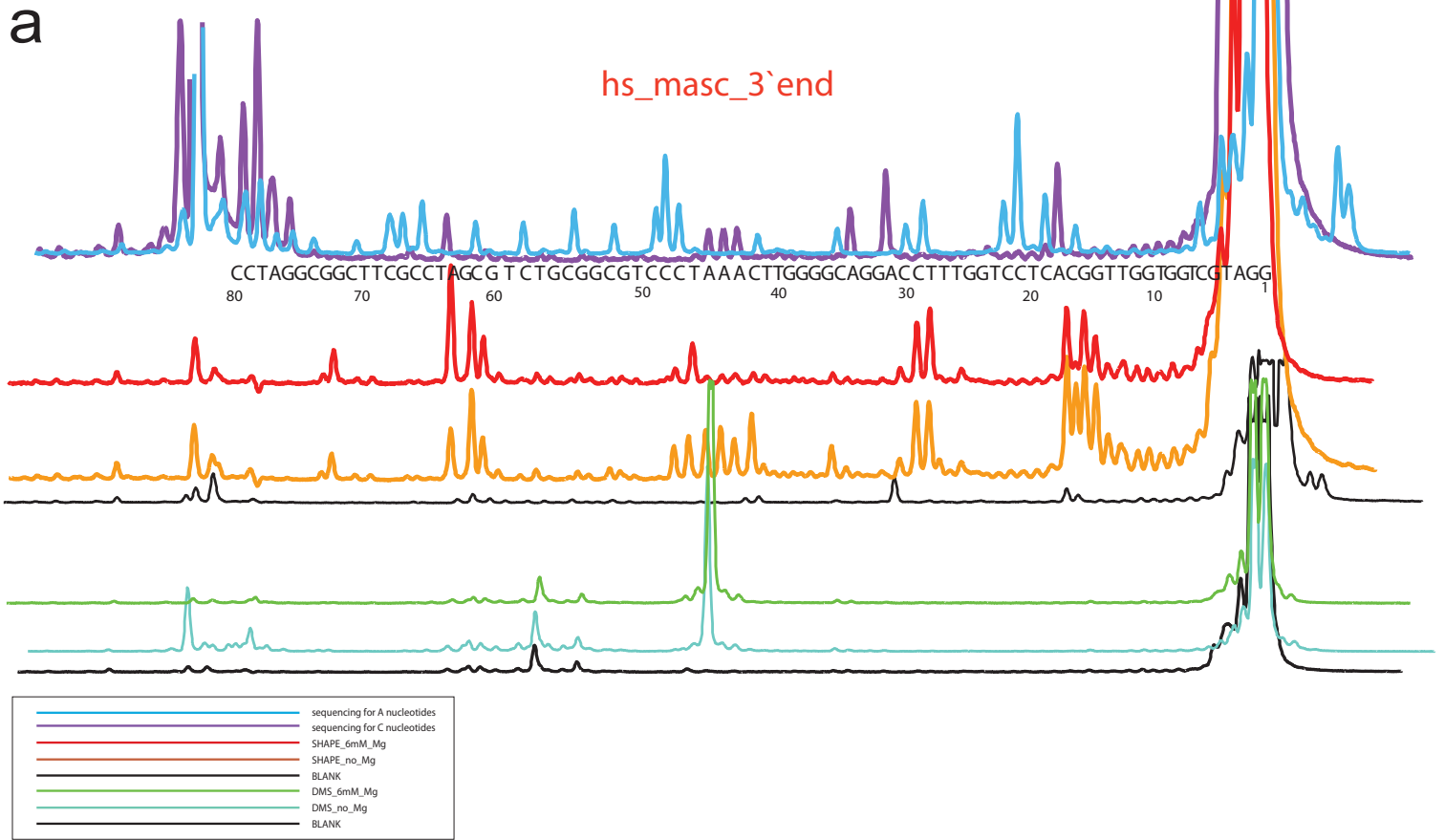


Figure S3: Human mascRNA forms a tRNA-like structure. Related to Figure 1  
 (a) SHAPE chemical probing of human mascRNA is consistent with the predicted tRNA-like structure. Capillary electrophoresis traces display nucleotides with low and high SHAPE reactivity, corresponding to low and high flexibility. Black, unmodified control; gold, SHAPE reactivity for 0 mM Mg<sup>2+</sup>; red, SHAPE reactivity for 6 mM Mg<sup>2+</sup>.  
 (b) Secondary structure, as determined by SHAPE and DMS probing experiments. Orange, high SHAPE reactivity; yellow, medium SHAPE reactivity; grey, low SHAPE reactivity; un-circled nucleotides, near-zero reactivity.

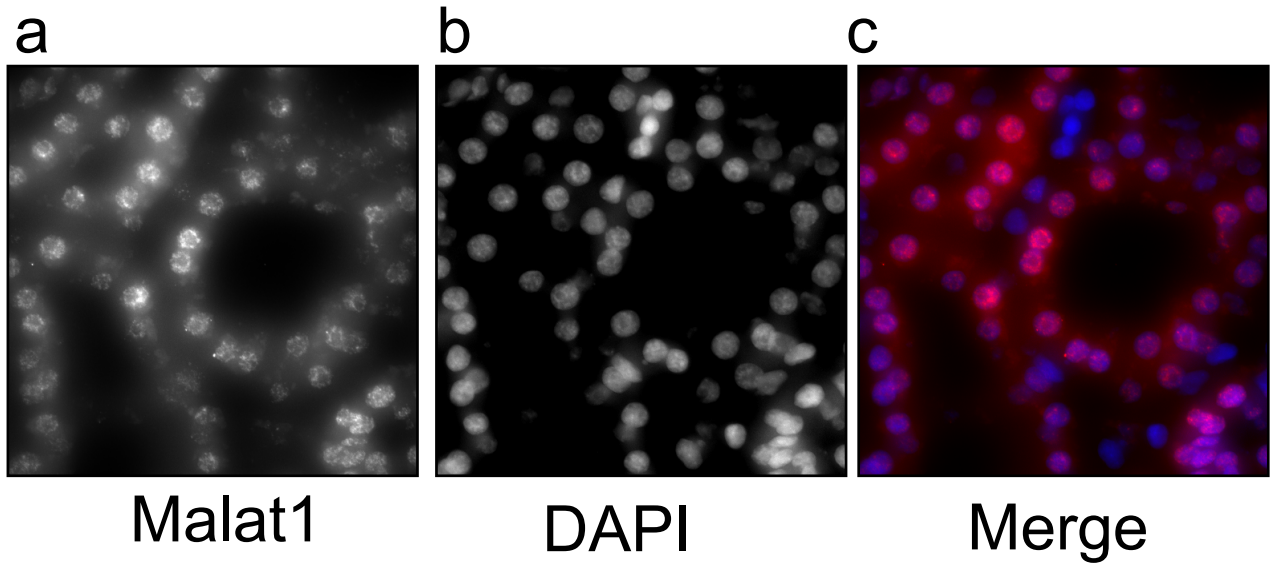


Figure S4: Lizard Malat1 RNA is enriched in nuclei in a punctate pattern. Related to Figure 2  
(a) RNA FISH using the Malat1 CDP probe (spectrum-red) shows that Malat1 is enriched in nuclei with a punctate pattern in adult lizard kidney (pseudocolor).  
(b) DAPI counter staining.  
(c) Merged image of a and b.

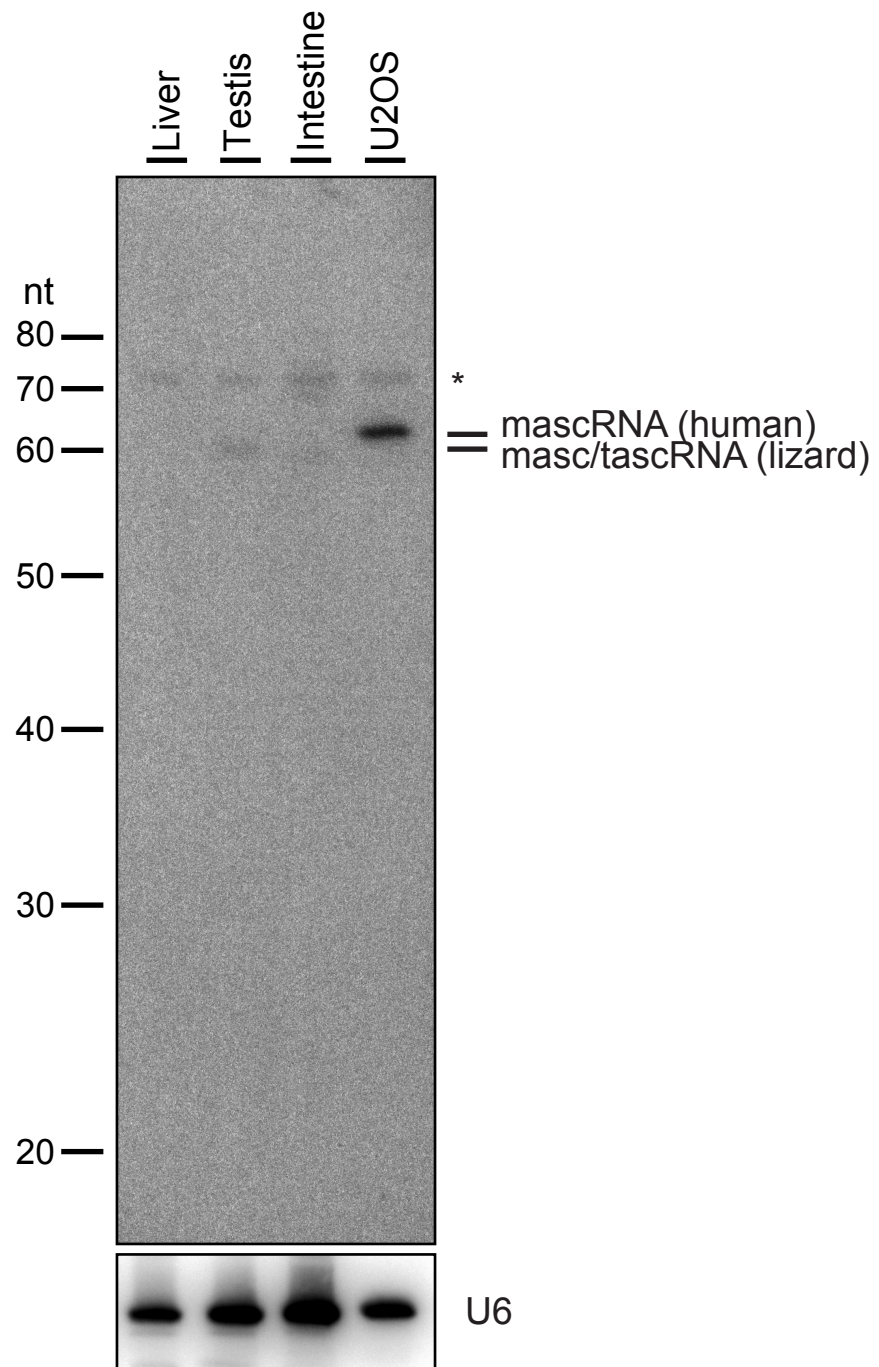
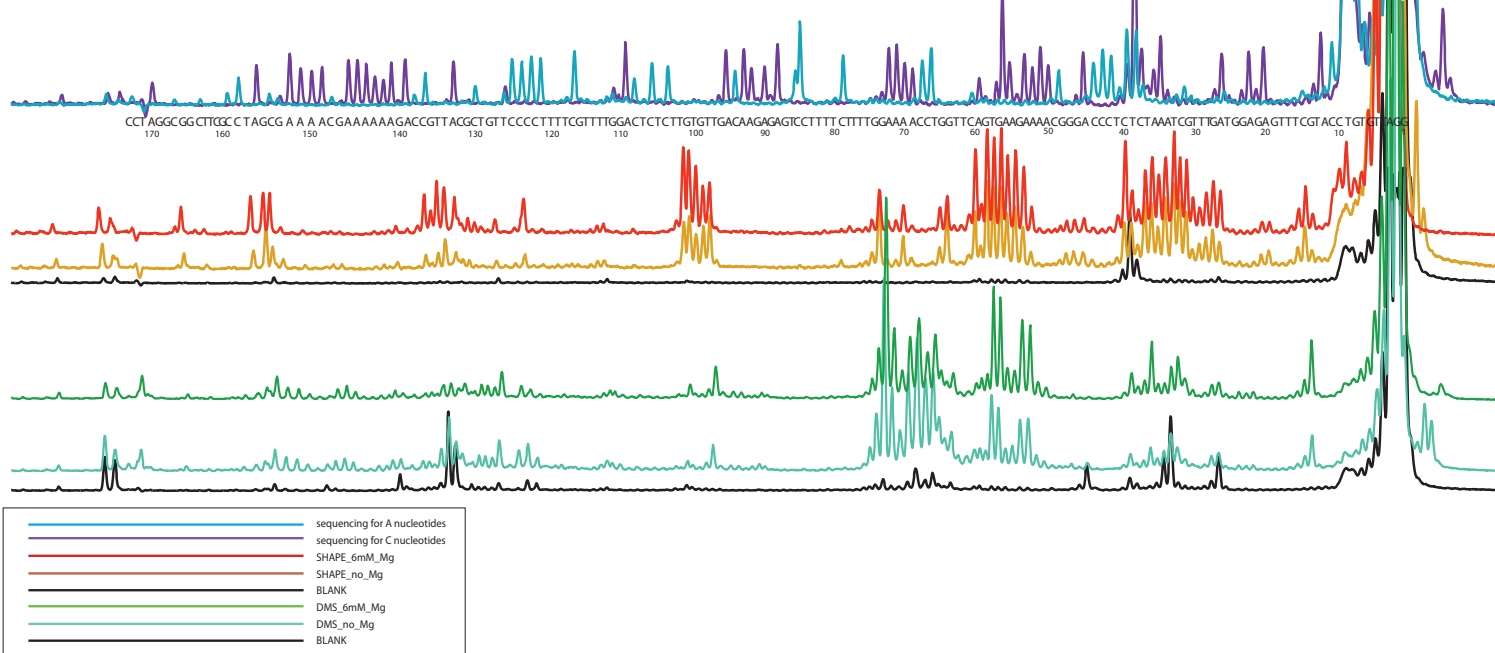


Figure S5: mascRNA/tascRNAs are produced from the 3' end of lizard Malat1 and tancRNAs. Related to Figure 2  
 Small RNA Northern blot analysis shows that the SRP probe (mascRNA/tascRNA antisense oligonucleotide probe) detects a strong signal of mascRNA in human U2OS cells (lane 4), a moderate signal of mascRNA/tascRNA in lizard testis (lane 2), a weak signal of mascRNA in lizard intestine (lane 3), and no signal of mascRNA in lizard liver (lane 1). Please note that lizard mascRNA/tascRNA (lanes 2 and 3) migrates slightly faster than human mascRNA. \*, a nonspecific band. U6 snRNA is the loading control.

a

lizard\_tanc\_3`end



b

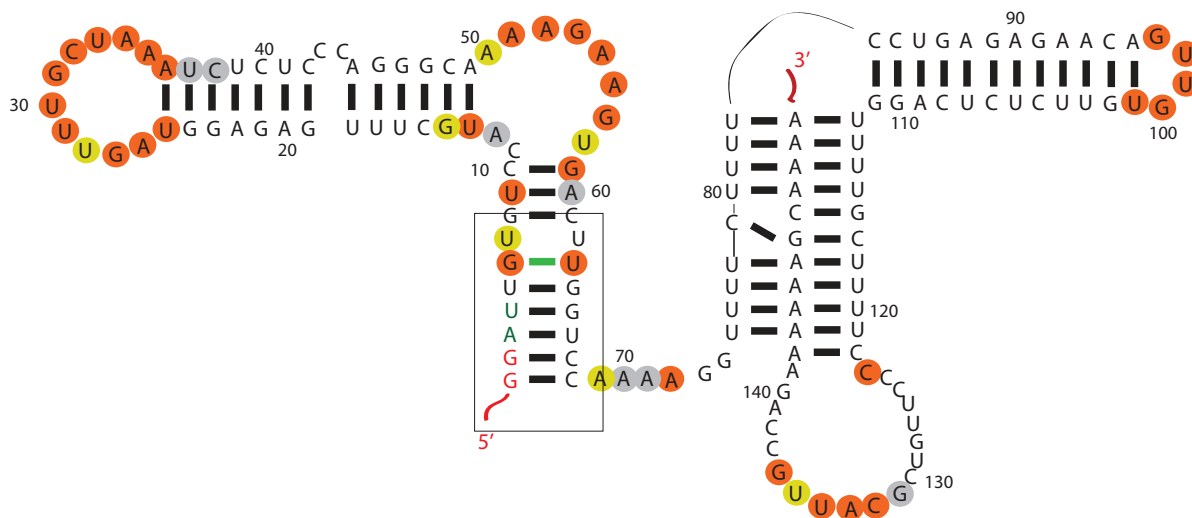


Figure S6. The 3' end of lizard tancRNA forms a triple helix structure. Related to Figure 5

(a) SHAPE chemical probing of the 3' end of lizard tancRNA is consistent with a triple helix. Capillary electrophoresis traces display nucleotides with low and high SHAPE reactivity, corresponding to low and high flexibility. Black, unmodified control; gold, SHAPE reactivity for 0 mM Mg<sup>2+</sup>; red, SHAPE reactivity for 6 mM Mg<sup>2+</sup>.

(b) Secondary structure, as determined by SHAPE and DMS probing experiments. Orange, high SHAPE reactivity; yellow, medium SHAPE reactivity; grey, low SHAPE reactivity; un-circled nucleotides, near-zero reactivity.

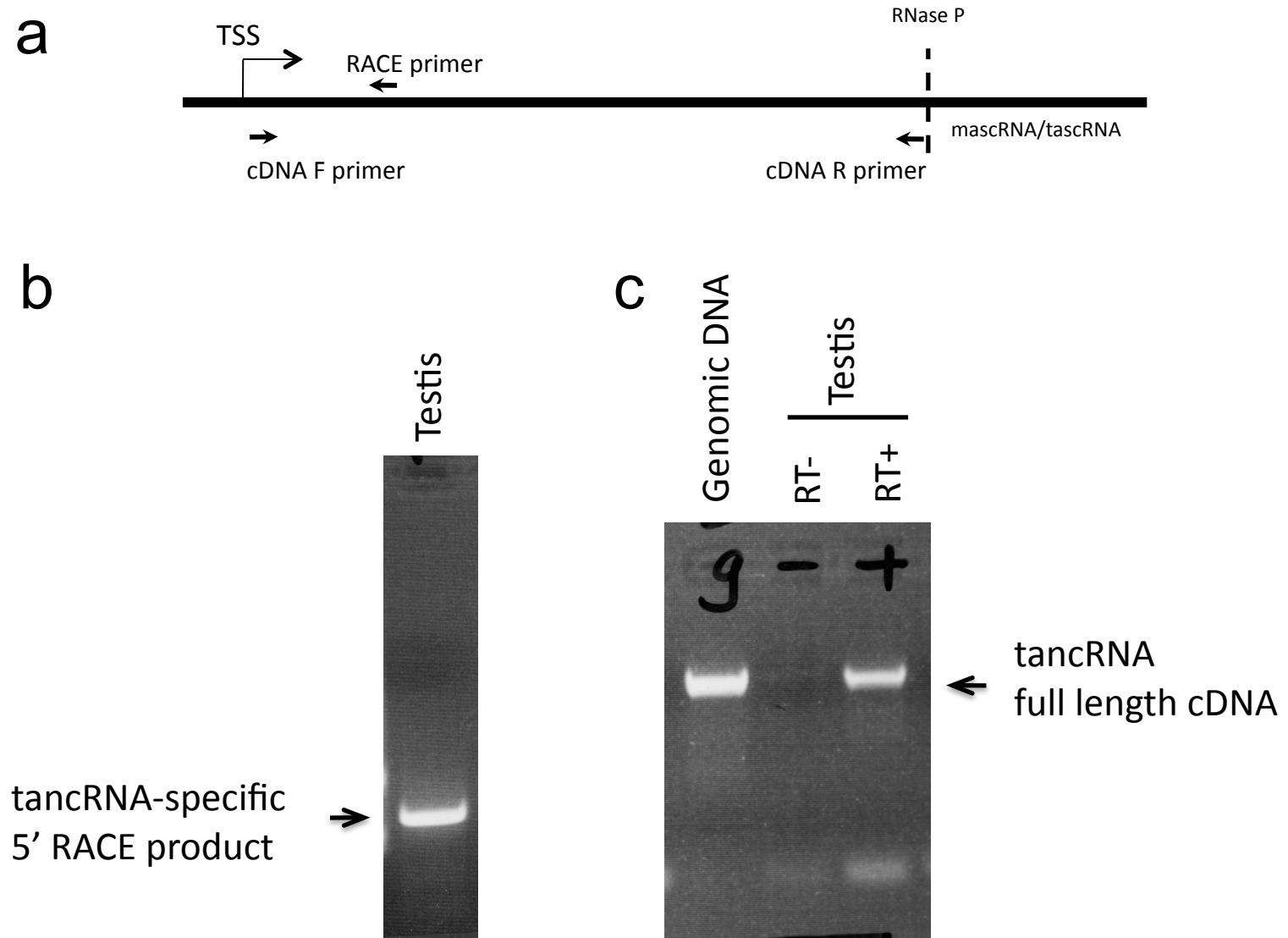


Figure S7. Lizard tancRNAs are capped at their 5' end. Related To Figure 5

(a) Schematic of the transcriptional unit of lizard tancRNAs. TSS, transcriptional start site; primers used for 5' Rapid Amplification of cDNA Ends analysis (5' RACE) and cDNA cloning are indicated.

(b) A 5' RACE product of tancRNA from the lizard.11 locus (see information in Supplementary File SF7) was run on 2% agarose gel.

(c) PCR amplification of the full length cDNA of tancRNA from the lizard.11 locus. The size of the tancRNA cDNA is the same as that of its corresponding genomic DNA, indicative of no splicing.

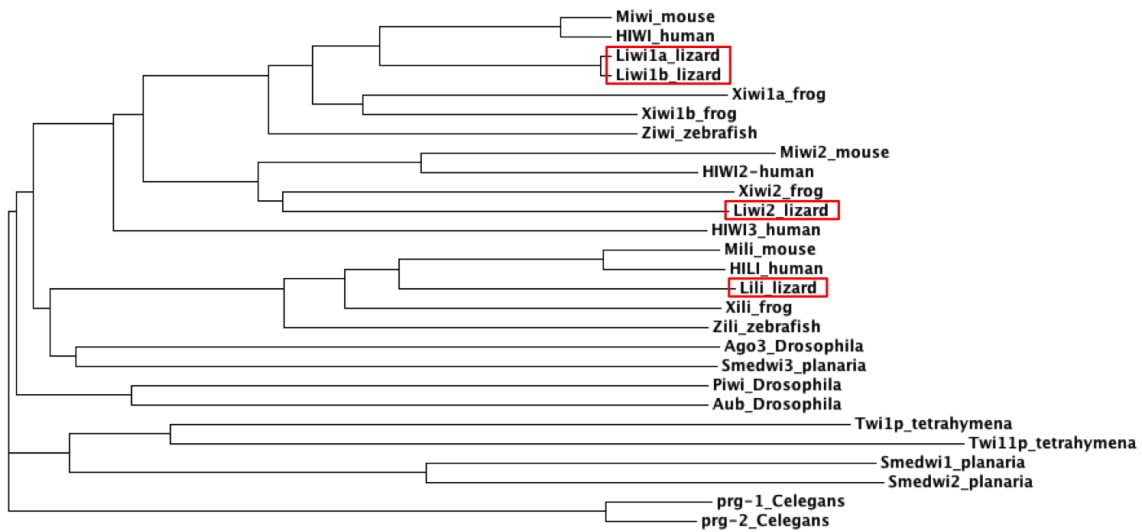
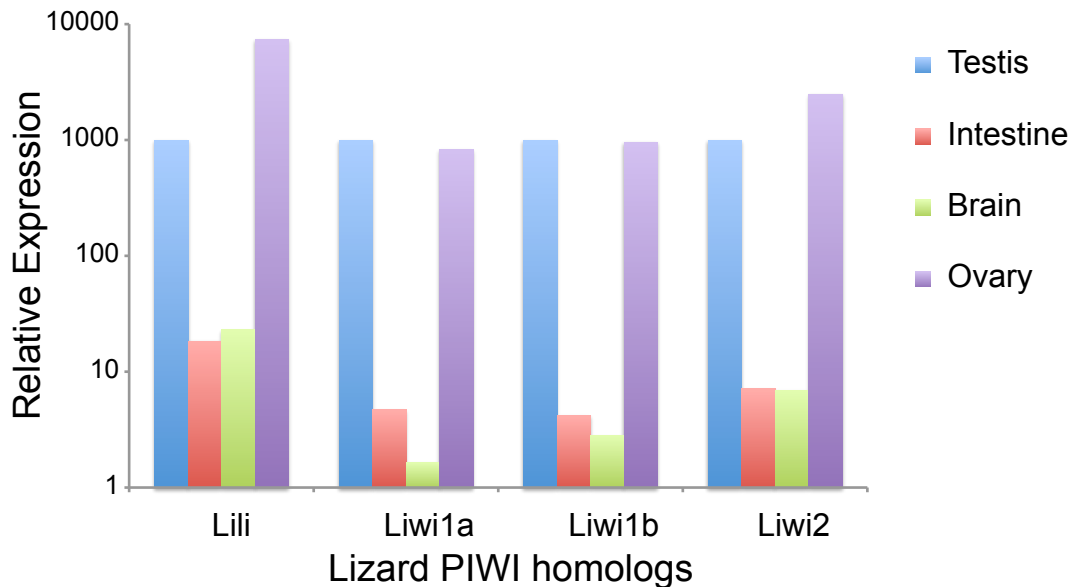
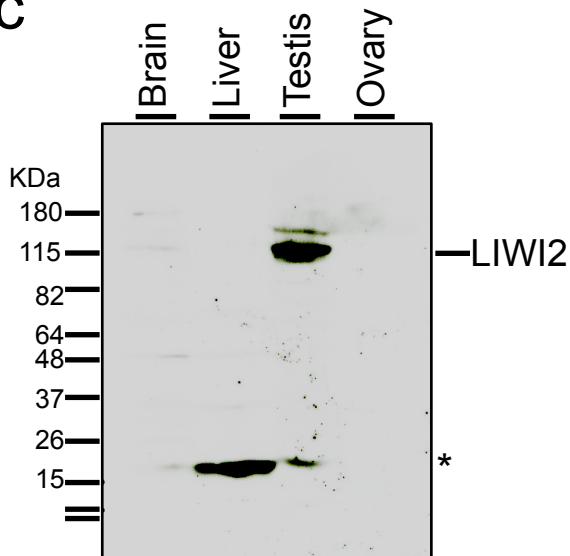
**a****b****c**

Figure S8. Four PIWI homologues are highly expressed in both testis and ovary of adult *Anolis carolinensis*. Related to Figure 7

(a) The phylogenetic tree of PIWI homologues. Four PIWI homologues, LILI, LIWI1a, LIWI1b, and LIWI2 are marked in red boxes.

(b) qRT-PCR analysis of RNA expression of PIWI homologues in adult lizard tissues. All PIWI homologues are expressed at high levels in lizard adult testis and ovary, but not in intestine and brain.

(c) Western blot analysis of LIWI2 in lizard adult tissues. LIWI2 protein is highly expressed in testis, but not in brain, liver, and ovary. Primers are listed in Supplementary File SF14.